Mycobacterium tuberculosis Erdman infection of cynomolgus macaques of Chinese origin

Jing Zhang[1,2], Ming Guo[2], Yan Rao[2], Yong Wang[2], Qiaoyang Xian[2], Qian Yu[2], Zhixiang Huang[2], Xin Wang[2], Rong Bao[2], Junqiu Yue[3], Zhijiao Tang[2], Ke Zhuang[2], Li Zhou[2], Zhuoya Li[1]

[1]Department of Immunology, School of Basic Medicine, Tongji Medical College, Huazhong University of Science and Technology, Wuhan 430030, China; [2]Animal Biosafety Level III Laboratory at the Center for Animal Experiment, Wuhan University School of Medicine, Wuhan 430072, China; [3]Department of Pathology, Hubei Cancer Hospital, Wuhan 430070, China

Contributions: (I) Conception and design: J Zhang, K Zhuang, L Zhou, Z Li; (II) Administrative support: Z Li; (III) Provision of study materials or patients: K Zhuang, L Zhou, Z Li; (IV) Collection and assembly of data: J Zhang, M Guo, Y Rao, Y Wang, Q Xian, Q Yu, Z Huang, X Wan, R Bao, L Zhou, J Yue, Z Tang; (V) Data analysis and interpretation: J Zhang, J Yue, Z Li; (VI) Manuscript writing: All authors; (VII) Final approval of manuscript: All authors.

Correspondence to: Zhuoya Li, MD, PhD. Department of Immunology, School of Basic Medicine, Tongji Medical College, Huazhong University of Science and Technology, Wuhan 430030, China. Email: zhuoyali@mails.tjmu.edu.cn.

Background: Nearly one-third of the population worldwide is estimated to have latent tuberculosis infection (LTBI), which represents a vast reservoir for a constant source of tuberculosis (TB) transmission. It has been suggested that cynomolgus macaques are less susceptible to *Mycobacterium tuberculosis* (*M.tb*) infection than rhesus macaques, we examined *M.tb* infection of Chinese cynomolgus macaques.

Methods: Eight Chinese cynomolgus macaques were infected with *M.tb* Erdman strain with a small [25 colony forming unit (CFU)] or large dose (500 CFU) via bronchoscopy. The infected animals were monitored for symptoms and examined by chest X-ray, computed tomography (CT), tuberculin skin test (TST), and enzyme-linked immunospot (ELISPOT).

Results: Based on TST conversion and the specific immune responses to *M.tb* antigens, all animals were successfully infected. Half of the animals developed active infection and died within 15 months postinfection. The other four animals were grouped with latent *M.tb* infection because of positive TST but few clinical signs and pathological changes of TB during the course of this study. Interestingly, a challenge with a large dose of *M.tb* also induced latent infection. Similar to the changes that occur with human TB patients, the animals with active infection exhibited weight loss, cough and typical TB pathological changes, including caseous granulomas, cavities, consolidation, lipid pneumonia, pleural effusion, lymphadenopathy and bacterial burden in lungs and other organs.

Conclusions: The low dose of *M.tb* was sufficient to cause both active and latent *M.tb* infection in cynomolgus macaques of Chinese origin.

Keywords: *Mycobacterium tuberculosis* (*M.tb*); non-human primate (NHP); Erdman strain; Chinese cynomolgus macaques; latent tuberculosis; active infection

Introduction

Tuberculosis (TB) is a leading cause of morbidity and mortality worldwide, with nearly 9 million new cases and 1.5 million deaths annually (1). The only vaccine widely used against TB, the mycobacterium Bacille Calmette-Guérin (BCG), shows variable efficacy against adult pulmonary TB disease and is unsuitable for people with an impaired immune system (2-4). Therefore, interventions must be improved, which requires relevant animal models for evaluation of the efficacy of novel vaccines and drug candidates against TB (5).

Non-human primates (NHPs) have been widely used to study a wide range of infectious diseases because of their close evolutionary relationship and biological relevance to humans (6,7). Macaques are excellent and attractive animal models for preclinical and clinical translational research on TB and have been extensively used to study the pathogenesis, vaccines and therapeutic interventions of TB, as these animal exhibit remarkable similarities to humans in almost every aspect of anatomy, genomes, physiology and immune systems (8). More importantly, macaque models can recapitulate the entire spectrum of possible infection outcomes and show similar disease presentation and complex pathological lesions to those observed in human *Mycobacterium tuberculosis* (*M.tb*) infection (9). Additionally, compared with other animals, macaques are the only models that reproduce a classic latent infection and TB/SIV co-infection (10).

Most of the work on the NHP model of *M.tb* infection has primarily used either the cynomolgus macaque of the Philippines (11-15) or the rhesus macaque of Indian origin (2,16). In several direct comparisons between these two species, cynomolgus macaques are relatively more resistant to *M.tb* infection than rhesus macaques. Rhesus show more extensive lung disease and extrapulmonary spread than cynomolgus after infection with the same dose of *M.tb* Erdman strain [3,000 colony forming unit (CFU)] (3). Additionally, our previous data revealed that rhesus macaques are highly susceptible to *M.tb* Erdman strain, developing active TB disease independent of the challenge dose (17). By contrast, several studies support that cynomolgus macaques are relatively more resistant to *M.tb*, showing the full spectrum of human TB including latent disease (11-13). However, the morbidity in the cynomolgus has more individual variation than that in rhesus infected with the same dose of *M.tb* (18). In this regard, cynomolgus macaques may provide potential advantage over rhesus monkeys for studying the pathogenesis of different disease states.

As a mainstay of NHP models in TB research, the availability of Philippine cynomolgus macaques has contributed greatly to our understanding of TB pathogenesis, precautions and therapy. However, TB is an infectious disease that affects people of diverse origins, and the animals used in the study of TB infection should also be considered for their genetic and geographical backgrounds. Cynomolgus macaques used for research typically come from large colonies in Asia or Indonesia and show substantial genetic diversity (19). Additionally, cynomolgus macaques from different origins are not interchangeable in the study of cellular immunity, particularly in TB vaccine research, because most MHC I alleles are found only in animals from a single geographic origin (19). Moreover, MHC also provides genetic control of susceptibility to infection. Therefore, whether cynomolgus of Chinese origin can represent the various outcomes resembling the human *M.tb* infection is unclear. In this study, we examined the susceptibility of cynomolgus macaques of Chinese origin to *M.tb* infection and found that a low dose of *M.tb* was sufficient to induce active or latent infection.

Methods

Experimental animals and ethics statement

Eight adult Chinese-origin female cynomolgus macaques at age from 4 to 5 years old were purchased from Hainan Non-human Primate Development of Laboratory Animal Co., Ltd., Hainan, China. These macaques were subjected to strict screening by the independent testing laboratory VRL Animal Health Services (AHS) to ensure that the animals were negative for four pathogens (simian retrovirus D, simian immunodeficiency virus, simian T leukemia virus type I, and herpes virus B). All animals were housed and maintained in the Animal Biosafety level-III (ABSL-III) laboratory, which is certified by the Association for Assessment and Accreditation of Laboratory Animal Care International. All housing and animal care procedures were in accordance with the Guide for the Care and Use of Laboratory Animals and Chinese law on animal experiments as previously described (17). The study manipulations and protocols were approved by the Institutional Animal Care and Use Committee of Wuhan University School of Medicine.

Pulmonary M.tb infection

Stocks of *M.tb* Erdman strain were obtained from the Food and Drug Administration (Bethesda, MD, USA). An aliquot was mixed and diluted in sterile saline to designed concentrations for infection. The animals were given experimental serial numbers (WAP01-WAP08), and naïve prior to infection on the ground of tuberculin skin testing (TST), interferon-γ (IFN-γ) enzyme-linked immunospot (ELISPOT) assays and thoracic radiographs. Each monkey was anesthetized with an intramuscular injection of ketamine hydrochloride (10 mg/kg) and atropine (0.04 mg/kg) and then infected bronchoscopically with 25 or 500 CFU of *M.tb* Erdman in the right lower lobe as described previously (17,20). After infection, all animals were individually housed in negative pressure cages (20,21). The re-defined humane endpoint was determined by the experienced veterinary staff based on a combination of the following clinical signs: loss of 25% peak post-infection weight, marked lethargy or persistent recumbency, excessive hypothermia, severe dyspnea at rest, and intractable pain or distress.

Clinical assessment

After inoculation, all animals were monitored and checked daily throughout the study for clinical signs of disease, including appetite, attitude, activity level, and cough, among others. The score systems of appetite and cough have been described previously (17). Appetite was scored by the amount of food taken per meal (2: all; 1: approximately half; 0: none). The maximum appetite score that an animal could achieve was 6 points per day and 42 per week, which was defined as 100%. A percentage of appetite score for each animal was calculated as weekly scores divided by 42. Cough score was also evaluated daily (0: no cough; 1: cough; regardless of cough frequency). The maximum cough score was 1 point per day and 7 points per week, which was defined as 100%. A percentage of cough score was calculated as weekly scores divided by 7. Animals were sedated to measure their weight and body temperature immediately before infection and at monthly intervals post-infection. Blood samples were collected for the erythrocyte sedimentation rate (ESR).

TST

To determine whether each animal was successfully infected,

0.1 mL of old tuberculin (OT) (Synbiltics Corporation, San Diego, California, USA) was intradermally administered into the palpebra of the right upper eyelid. The same volume of sterile saline was injected into the left eyelid as a negative control. A veterinarian using a standardized grading system then evaluated the palpebral reaction at 24, 48 and 72 h, as previously described (17).

ELISPOT assays for M.tb-induced IFN-γ releases

ELISPOT assay (U-Cytech Biosciences, Utrecht, The Netherlands) was performed as previously described (21). Briefly, plates (Millipore Corp., Bedford, MA, USA) were coated with anti-human/macaque IFN-γ monoclonal antibody overnight at 4 ℃. Peripheral blood mononuclear cells (PBMCs) were isolated from fresh blood and then added into the plates at 3×10^5 cells/well. Cells were stimulated in duplicate with PPD (10 µg/mL), ESAT-6 (0.5 µg/mL), CFP-10 (0.5 µg/mL) or rAg85a (0.5 µg/mL; kindly gifted by Aeras) from *M.tb* or concanavalin A (ConA, 5 µg/mL, Sigma, St. Louis, MO, USA) and then incubated for 18 h. ELISPOT medium served as a negative control. An ELISPOT reader (Bioreader 4000; BIOSYS, Germany) counted the number of spots, and data were expressed as the number of spot-forming units (SFUs) per million PBMCs.

Chest X-ray and CT scanning

Thoracic radiographs of all macaques were performed with a digital X-ray unit (SIEMENS Multimobil 2.5 Mobile 810 DDR system and PiView STAR WorkStation System) before inoculation, monthly PI and at the time of the necropsy. A CT scan was performed in an Animal Biosafety Level III Laboratory using a high-resolution cone beam CT system (Fidex veterinary imaging system; Animage LLC, California, USA). Two experienced thoracic radiologists in a double-blind manner interpreted all X-ray and CT images.

Necropsy

Pathologists with extensive nonhuman primate experience for *M.tb* infection performed complete necropsies as described previously (17). The animals were anesthetized with ketamine (i.m. 10 mg/kg), followed by an intravenous overdose of sodium pentobarbital (100 mg/kg) and immediate necropsy. Multiple tissue specimens with gross lesions from *M.tb*-infected macaques were harvested, including lobes of each lung, bronchi, lymph nodes, livers,

3612

Zhang et al. TB infection of Chinese-origin cynomolgus macaques

spleens and kidneys. Gross examinations that included but were not limited to the presence, localization, number, size, and pattern of lesions were conducted. A relative pathology scoring system was used to calculate TB lesions in the organs from infected animals (13,22).

Histopathological analysis

Tissue samples used for histopathological examination were removed randomly from the lung lobes, lymph nodes, livers and spleens of *M.tb*-infected animals. These tissues were fixed in 10% formalin, routinely processed, and embedded in paraffin. Sections 4 µm thick were cut, stained with hematoxylin and eosin (HE) and selectively with the Ziehl-Neelsen method. The histopathological changes were then observed under a microscope (AXIOSKOP 40; Zeiss, Germany).

Immunohistochemistry

Paraffin sections 4 µm thick were stained with the streptavidin-peroxidase immunohistochemical technique after heat-induced antigen retrieval in citrate buffer. The sections were incubated for 60 min at room temperature with a monoclonal antibody specific to thyroid transcription factor-1 (TTF-1) (ZM-0270, clone SPT24; ZS Biotechnology Company), followed by biotin-conjugated secondary antibody against IgG (Beijing Zhongshan Biotechnology). After washes, the sections were then incubated with peroxidase-labeled streptavidin for 20 min and color was developed by incubation with its substrate diaminobenzidine. TTF expression was observed under a microscope.

Bacterial burden (17,21)

Tissue specimens were minced and homogenized in phosphate buffered saline (PBS) by a tissue mixer homogenizer (PRO 250; PRO Scientific, Monroe, CT, USA). All samples were serially 10-fold diluted in PBS before being plated onto Middlebrook 7H11 medium (Difco, BD, USA) plus OADC supplements (Difco) and cycloheximid (100 µg/mL; Sigma, St. Louis, MO, USA). After spreading the homogenate solution, plates were incubated at 37 ℃ in an incubator for 3–5 weeks and then formed colonies were counted.

Statistical analyses

Data were analyzed using Graphpad Prism version 6.0 (Graphpad Software, San Diego, CA, USA) and the SPSS statistical software package (version 16.0, SPSS, Chicago, IL, USA). The differences in the clinical evaluations and IFN-γ release were analyzed using the Mann-Whitney test. P values <0.05 were considered statistically significant.

Results

Different susceptibility of cynomolgus macaques of Chinese origin to infection with low dose of M.tb

To determine the susceptibility of cynomolgus macaques of Chinese origin to *M.tb* infection, we infected animals with a small dose (25 CFU) of *M.tb* and a large dose (500 CFU), a standard dose served as a positive control, to induce TB (23,24). Our results showed that infection with the small dose of bacteria induced active disease in 50% of animals and latent status in the others, which had no clinical or radiographic findings of disease for at least 6 months. Unexpectedly, the infection with the large dose of *M.tb* did not induce active disease in all animals but caused a latent infection in one of two animals in our experimental system (*Figure 1A*). The survival curves revealed that three of four animals with active infection died of advanced pulmonary TB disease in 32, 36 and 63 weeks after *M.tb* infection (*Figure 1B*); however, the animal that received 500 CFU of *M.tb* Erdman survived longer than those inoculated with 25 CFU of bacteria and was the one alive after more than 15 months, although with obvious clinical signs of active TB disease.

General clinical symptoms and features after M.tb infection

The most common and systemic symptoms of *M.tb* infection in humans are chronic dry cough, low-grade fever and loss of appetite and weight. Consistently, the four animals with active infection exhibited loss of appetite and body weight to a varying degree, compared with those with latent infection (*Figure 2A,B*). In particular, the two animals that died the earliest showed obvious appetite loss from 22 weeks after infection and lost approximately 14% and 13% of their total body weight before death (*Figure 2B*). The animal infected with the large dose of bacteria had significant anorexia as early as the second week and weight loss up to 17% at 32 weeks after infection. By contrast, the animals with latent infection showed little change in appetite (transient minor loss of appetite observed
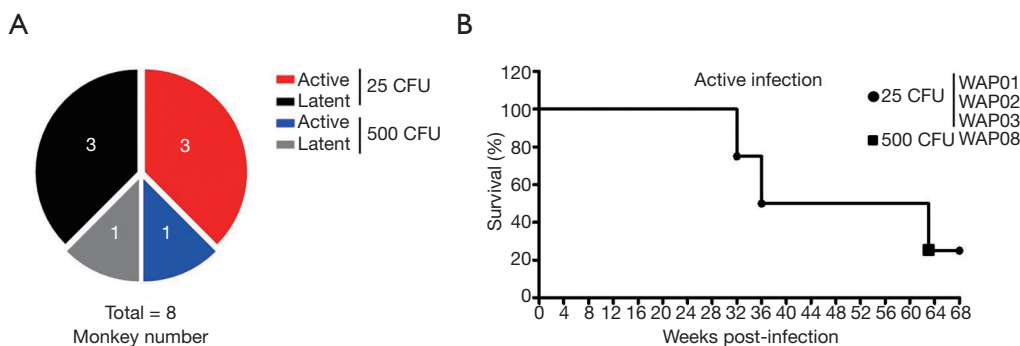
Figure 1 Survival of animals infected with *M.tb* Erdman strain. (A) Eight animals were challenge by bronchoscope with 25 CFU (n=6) or 500 CFU (n=2) of *M.tb* Erdman strain; (B) survival time of animals with active infection after inoculation with *M.tb* Erdman strain. *M.tb*, *Mycobacterium tuberculosis*; CFU, colony forming unit.
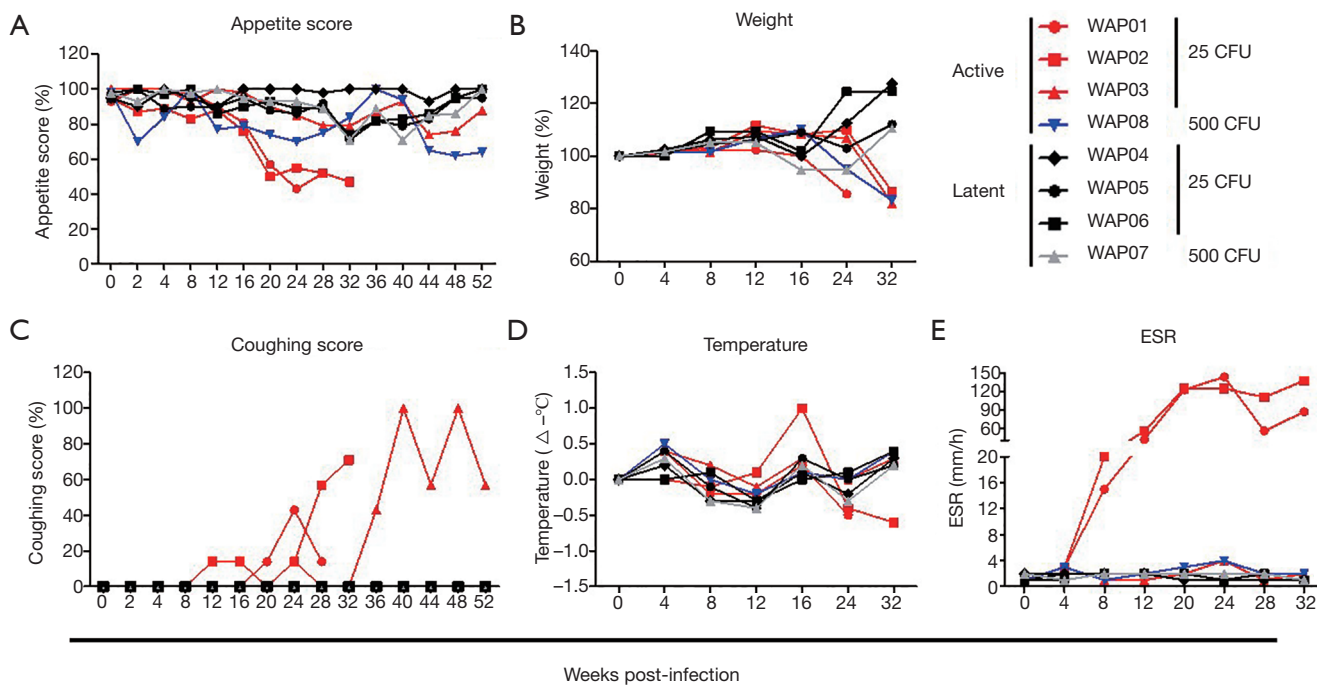

Figure 2 Clinical manifestations of animals infected with *M.tb* Erdman strain. Eight animals were bronchoscopically inoculated with 25 CFU (n=6) or 500 CFU (n=2) of *M.tb* Erdman strain. (A) Weekly appetite score; (B) percentage of body weight before inoculation; (C) weekly coughing score; (D) body temperature changes (subtract temperature value before inoculation); (E) ESR. *M.tb*, *Mycobacterium tuberculosis*; CFU, colony forming unit; ESR, erythrocyte sedimentation rate.

in only two animals) and experienced a weight gain of 11–27% at 32 weeks. Additionally, among animals with active infection, only the three infected with the small dose of *M.tb* had cough symptoms starting from 12–24 weeks that persisted throughout the study, whereas the animal infected with the large dose of bacteria did not cough, even when radiographic findings of disease were observed

(*Figure 2C*). Although nearly all animals had fluctuating temperatures in the normal range after *M.tb* infection, a low fever (1 ℃ above the base level) was observed at 16 weeks post-infection in only one of the two animals that died early (*Figure 2D*). ESR is one of the inflammatory markers contributing to the diagnosis of active *M.tb* infection. Only in the two animals that died earliest, ESR levels were
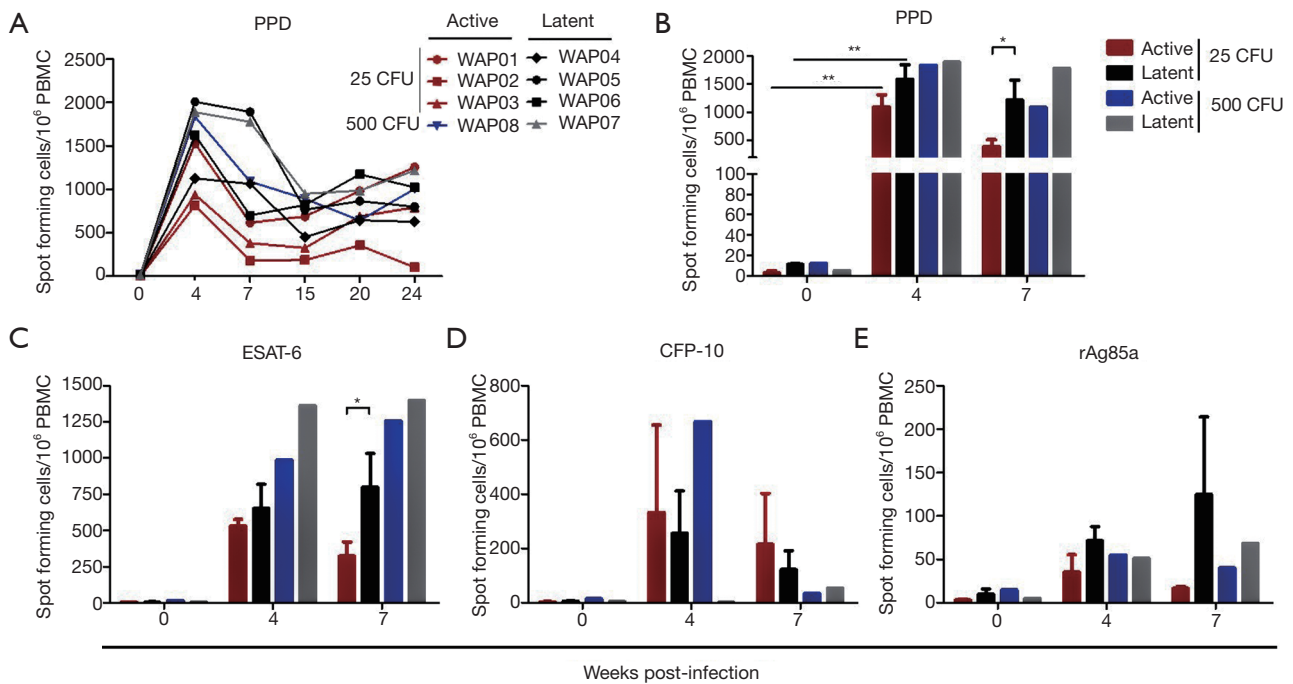
3614

Zhang et al. TB infection of Chinese-origin cynomolgus macaques

Figure 3 IFN-γ release during *M.tb* infection. *M.tb* antigen-specific IFN-γ production was measured in PBMCs from monkeys stimulated for 18 hours with PPD (10 μg/mL), ESAT-6 (0.5 μg/mL), CFP-10 (0.5 μg/mL), or rAg85a (0.5 μg/mL) using the ELISPOT assay. Numbers of *M.tb* antigen specific IFN-γ containing spots are shown as SFU/10^6 cells. (A) Frequency of PPD-specific IFN-γ-secreting cells during *M.tb* infection; (B-E) IFN-γ production in response to PPD (B), ESAT-6 (C), CFP-10 (D) or rAg85a (E) at 0, 4 and 7 weeks PI. Data from animals with latent (n=3) or active infection (n=3) of the 25 CFU M.tb Erdman strain treatment are represented as the mean ± SEM. *P<0.05, **P<0.01. *M.tb*, *Mycobacterium tuberculosis*; CFU, colony forming unit; IFN-γ, interferon-γ; PBMC, peripheral blood mononuclear cell; ELISPOT, enzyme-linked immunospot; SFU, spot-forming unit; SEM, standard error of mean; PI, post-infection.

elevated as early as 8 weeks and reached peaks at 24 and 32 weeks after infection, whereas in the other animals with active or latent infection, ESR levels remained unchanged during the course of *M.tb* infection (*Figure 2E*).

TST and IFN-γ release assay

A combined two-step diagnostic approach is recommended for tuberculosis infection, which includes initial screening with TST followed by a subsequent IFN-γ release assay (particularly when a TST may be unreliable) to confirm TST results, based on the tuberculosis guidelines from the UK National Institute for Health and Clinical Excellence. In this study, TST was performed at 18 weeks after *M.tb* inoculation to confirm successful infection. The right eyelid of animals was injected with OT; whereas the left eyelid was used as a negative control. Based on our results, all animals

that received the *M.tb* Erdman strain had a positive skin test with grade 4; thus, the degree of positive TST reactions among the monkeys was same regardless of the challenging dose of *M.tb* and different disease status.

IFN-γ ELISPOT was performed to determine changes in the frequency of IFN-γ-producing PBMCs. As expected, the number of PPD-activated and IFN-γ releasing cells increased sharply in all monkeys at 4 weeks post-infection (*Figure 3A,B*), but the latent animals had a tendency to release more IFN-γ than active ones infected with the low dose of *M.tb*, particularly at 7 weeks post-infection (*Figure 3B*). A similar phenomenon was observed in active or latent TB of monkeys in response to a single challenge of *M.tb*-specific antigen ESAT-6 (*Figure 3C*), but not to a single challenge of CFP-10 (*Figure 3D*) or rAg85a (*Figure 3E*). These data indicated that IFN-γ production was beneficial for the animals against TB, at least in response to the low dose of *M.tb*.
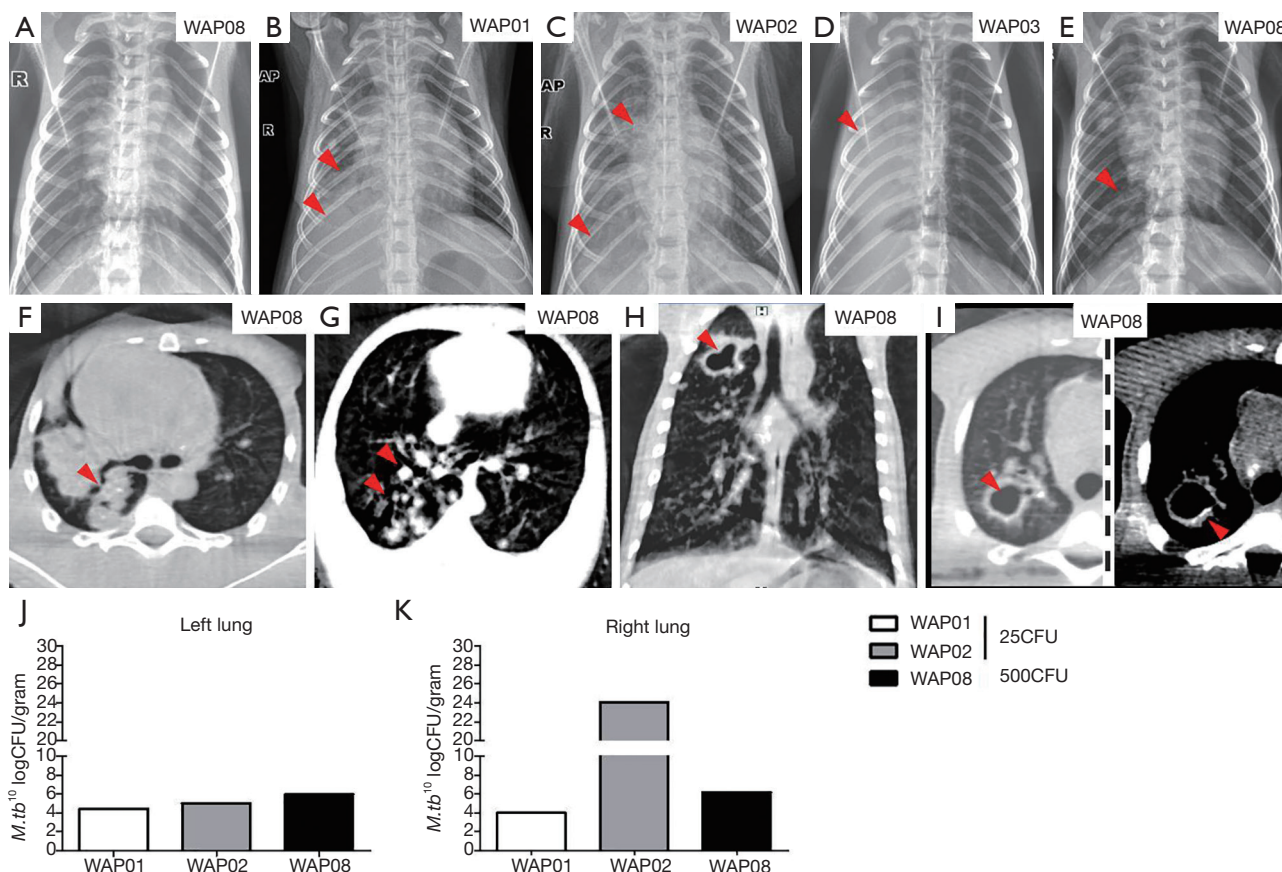
Figure 4 Chest radiology and bacterial burdens in the lungs from *M.tb*-infected animals. (A) Normal chest film of animal WAP08 before infection; (B-E) chest radiographs of four animals with advanced pulmonary mycobacterial infection. The right side of the monkey is marked on radiographs as "R," and the arrows indicate lesions; (F-I) CT images of animal WAP08 with active infection; (H,I) cavitation in the right upper lung lobe with calcified wall (left is lung window, and right is mediastinum window in I; the arrows indicate lesions); (J,K) bacterial burden was measured in CFU per gram in the left (J) and the right (K) lung lobes at necropsy of animals with active infection. *M.tb*, *Mycobacterium tuberculosis*; CFU, colony formation unit.

Chest X-ray and CT evaluation of pulmonary lesions during disease development and bacterial burden in the lungs of infected animals

The radiographs demonstrated a steady progression of disease in all animals with active infection. Baseline chest films of all animals were negtive before infection (*Figure 4A*). Three of four animals with active disease initially showed pneumonia in the right lower lobe at 8, 15 and 32 weeks post-infection, characterized as small focal areas of pneumonia with nodularity or multiple patches and pleural effusion (*Figure 4B,C,D*). Additional findings (*Table 1*) included consolidation (*Figure 4C,D*), atelectasis (*Figure 4D,E*), emphysema (*Figure 4D*) and the development of cavitation (*Figure 4E*). Notably, the last animal with active

infection had negative chest radiographs for more than 28 weeks and then displayed atelectasis in the right lung lobes at 32 weeks and emphysema in the left lobe at 46 weeks post-infection (*Figure 4E*). Animals with latent infection had negative chest X-ray films throughout the study.

Chest radiography is the most useful tool for evaluating lung infection and plain film results are sufficient for tuberculosis diagnosis in most cases. However, CT is more sensitive than plain film for the detection of lung lesions and enlarged lymph nodes. For example, CT showed a nodule in the left lobe, whereas the chest radiograph showed no evidence of nodularity lesions in the lobe. Similar to human TB disease, a variety of characteristic CT findings of

3616

Zhang et al. TB infection of Chinese-origin cynomolgus macaques

Table 1 Disease features of chest X-ray in cynomolgus macaques infected with *M.tb* Erdman strain

Group	Solitary nodule	Mass	Consolidation	Cavity	Lymphadenopathy	Pleural abnormality	Atelectasis	Emphysema
25 CFU								
Active	3/3	3/3	1/3	0/3	0/3	2/3	1/3	1/3
Latent	0/3	0/3	0/3	0/3	0/3	0/3	0/3	0/3
500 CFU								
Active	1/1	1/1	1/1	1/1	0/1	1/1	1/1	0/1
Latent	0/1	0/1	0/1	0/1	0/1	0/1	0/1	0/1

Number of macaques showing TB feature/total number in group. *M.tb, Mycobacterium tuberculosis*; TB, tuberculosis.

tuberculosis involved in the thoracic were observed in this study. Typical CT findings in the bronchogenic spread of pulmonary tuberculosis were observed, such as centrilobular branching linear lesions with multiple micronodules, and the large area of consolidation in the posterior segment of the right lung (*Figure 4F*). CT images also showed multiple branches with terminal clubbing, called "tree-in-bud" appearance (*Figure 4G*), and a large, irregular and thick-walled cavity with calcification in the right lung lobe from one animal at 42 weeks post-infection (*Figure 4H,I*), which both indicated active disease.

Bacterial counts demonstrated *M.tb* growth in all lung tissues of the animals with active disease. The bacterial burdens in animals challenged with the high dose of *M.tb* were not higher than those in animals challenged with the low dose *M.tb*, either in the left or right lung (*Figure 4J,K*). Additionally, right lungs (inoculation site) did not contain higher bacterial numbers than left lungs except in WAP02. The animals with latent infection remained alive and bacterial cultures were not performed.

Intrapulmonary pathological lesions of animals with active infection

Three of four infected monkeys were euthanized because of advanced disease. Necropsy revealed extensive adhesions among right lung lobes and adjacent thorax tissues, such as the pericardium and diaphragm, in these animals. Multiple coalescing caseous granulomas up to 1.5–2.0 cm in diameter were observed. By contrast, some scattered nodules without adhesions occurred among the lobes and thorax in left lungs. Additionally, consolidation, lipid pneumonia, pleural effusion, peritoneal fluid and cavities were also observed.

Similar to human TB disease, animals with active infection exhibited somewhat different types of granulomas.

We observed a small number of solid granulomas composed largely of lymphocytes and epithelioid macrophages without central necrosis (*Figure 5A*). In both right and left lobes, necrotic granulomas were mostly observed, which is a type of granuloma that contained a demarcated central necrotic region caused by death of infected cells (*Figure 5B*). Additionally, multifocal and confluent caseous granulomas were most commonly observed in the right lung lobes. These lesions were composed of large areas of central caseation necrosis caused by liquefaction of dead cells, surrounded by epithelioid macrophages and rare giant multi-nucleated cells, with peripherally located lymphocytes and neutrophils (*Figure 5C*). A few of the lesions showed calcification changes in the central caseous region (*Figure 5D*). Necrotic granulomas even entered into the bronchial lumen (*Figure 5E*). Pulmonary cavities were observed in two animals that likely resulted from erosion of caseating granulomas into bronchi (*Figure 5F*). Moreover, we also observed a caseous granuloma invading into the vascular wall in the right lung of an animal, which suggested *M.tb* dissemination from blood (*Figure 5G*).

Inflammation is the most common feature of developing TB disease. Animal WAP01 showed acute inflammation of the entire lung, which was characterized by alveoli filled with exudate and infiltrated foamy macrophages and with deposition of fibrinous materials (*Figure 5H*). Except for the acute inflammation in the right lung lobe animals WAP02 and WAP08 exhibited chronic inflammation in the left lung, demonstrated by thickening of alveolar septa and ecchymosis in the microvascular area (*Figure 5I*). Additionally, we found consolidation in the right middle lung lobe (*Figure 5J*) in animals WAP02 and WAP08, whereas no evidence of consolidation and cavities was observed in WAP01. Reactive hyperplasia of type II alveolar pneumocytes was also observed in the right upper lung and
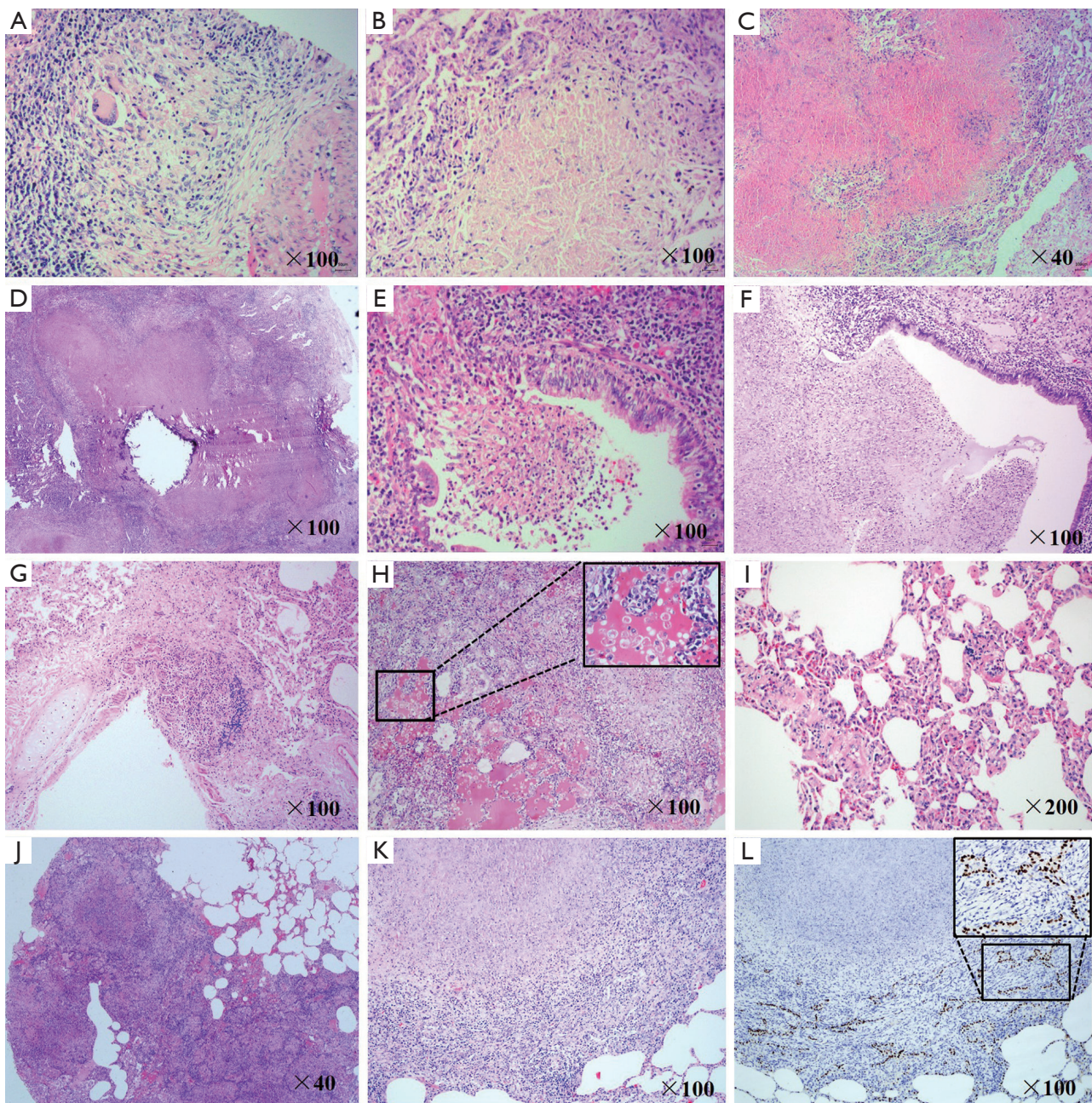
Figure 5 Histopathologic changes of *M.tb*-infected lungs. (A-K) Lung sections were stained with HE-staining. (A-D) Different granulomas in the lung of WAP08 (A, B, D) and WAP01 (C). (E,G) Invasion of granulomas into bronchial lumen (WAP02) and blood vessel (WAP01). (F) A cavity containing necrotic lung tissue (WAP02). Acute inflammation in the right lung (H) and chronic inflammation in the left lung (I) of WAP02. (J) Consolidation in the right middle lung lobe (WAP08). Alveolar epithelial cell hyperplasia in the right lung lobe of WAP02 (K), which was further confirmed by immunohistochemistry staining with thyroid transcription factor-1 (L). *M.tb*, *Mycobacterium tuberculosis*.
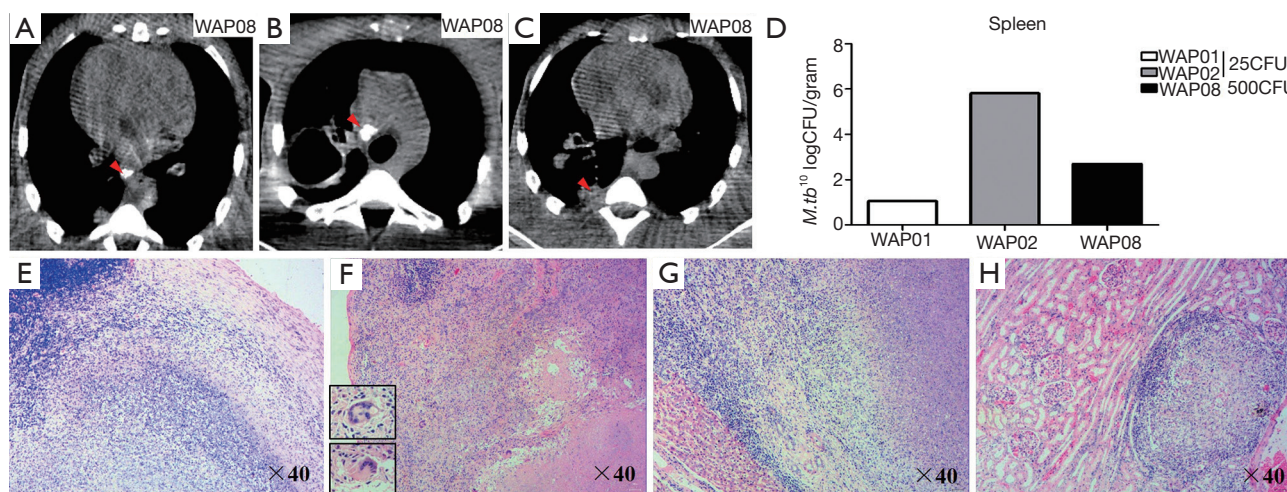
3618

Zhang et al. TB infection of Chinese-origin cynomolgus macaques

Figure 6 Extrapulmonary changes of animals with active infection. (A-C) CT images of *M.tb*-infected extra-thoracic organs (WAP08). (A) Subcarinal lymphadenopathy (arrow) and calcified node; (B) mediastinal lymphadenopathy (arrow) and calcified node; (C) pleural thickening and adhesion (arrow); (D) bacterial burdens in the spleens of animals with active infection; (E-H) histopathologic changes of *M.tb*-infected extra-thoracic organs; (E) caseous granulomas in hilar lymph nodes (WAP01); (F) caseous granulomas in spleen (WAP01); (G) caseous granulomas in liver (WAP02); (H) lymphocytic cuff around the solid granuloma in the kidney (WAP02). *M.tb*, *Mycobacterium tuberculosis*.

left lower lung from animal WAP02 (*Figure 5K*). Using immunohistochemistry, this result was further confirmed in stained cells by an antibody specific to TTF-1, a specific marker of hyperplastic alveolar cells caused by chronic lung (*Figure 5L*).

Extrapulmonary pathologic lesions in animals with active infection

Mediastinal or subcarinal lymphadenitis is a frequent manifestation of tuberculosis, with the right paratracheal node preponderantly involved in human TB disease. Enlarged and calcified subcarinal and mediastinal lymphadenopathy was observed in cynomolgus macaques (*Figure 6A,B*). Additionally, pleura thickening and adhesions (*Figure 6C*), with or without effusion, were observed in different animals on CT scans. In the necropsies of the animals with active infection, lymphadenopathy was found in the inguinal, axillary, hilar, and/or subcarinal nodes. Furthermore, bacteria also grew in the spleen, as in the lung, of animals with active infection (*Figure 6D*). Extra pulmonary *M.tb* infection was observed in the lymph node (*Figure 6E*), spleen (*Figure 6F*), liver (*Figure 6G*) and kidney (*Figure 6H*), showing solid and caseous granulomas in these organs in animals WAP01 and WAP02. Similar to the intrapulmonary pathological changes, multifocal and coalescing caseous

granulomas were commonly observed in animal WAP01, whereas scattered caseous granulomas with a necrotic central core were often observed in animal WAP02.

Discussion

In the present study, we provide compelling evidence that cynomolgus macaque is highly susceptible to *M.tb* Erdman strain infection. All the animals were infected with Erdman strain *M.tb* via intrabronchial instillation in a low or a high dose. Successful *M.tb* infection was confirmed in all eight animals by conversion of negative to positive TST and PBMC ELISPOT assays. Of the eight monkeys infected with *M.tb*, progression patterns of the disease were different. Based on clinical signs, radiographs, microbiologic cultures and necropsy findings, four animals (WAP01, WAP02, WAP03 and WAP08) were grouped with active disease, whereas the other four were grouped with latent infection. The animals with active infection showed similar manifestations of *M.tb* infection to those of humans, including anorexia, weight loss, positive TST, and elevated ESR, during the course of the infection. By contrast, animals with latent infection survived without any signs of the disease for more than 18 months, although these animals were also TST-positive. This is consistent with the clinical definition of humans with latent *M.tb*

infection (25) and that the grade of TST-positive reaction is unrelated with outcomes and severity of the disease. Two of the eight animals inoculated with the high dose of 500 CFU of *M.tb* were intended for use as positive controls, because this dose consistently induces severe active TB in all macaques (23,24). However, unexpectedly, a latent infection was induced in one of these animals with no radiographic changes and no clinical signs of disease for at least 6 months. It should be noted that, the earliest lesions of macaques with active TB occur in the right lower lobes (inoculation site) other than in the apical and posterior segments of the upper lobes observed in clinical patients. It is the result of different route of exposure.

IFN-γ is considered an essential cytokine for the control TB. Notably, the animals that were eventually diagnosed with latent TB had a tendency to release more IFN-γ than those that developed active TB, although this result only occurred in the group infected with the low dose of bacteria at 7 weeks post-infection. Additionally, the similar phenomenon was observed in active or latent TB of monkeys in response to a single challenge of the *M.tb*-specific antigen ESAT-6. By contrast, Lin *et al.* showed that macaques that would develop active disease released more IFN-γ than animals with latent TB (26). This discrepancy could be due to the differences in macaque species used in the studies or different time points for the testing. Notably, at the time when active-TB macaques showed signs of disease, no statistical differences were detected in the frequency of IFN-γ secreting cells between actively and latently infected monkeys in response to any of the antigens. These findings support the reports from population-based data (27,28) and suggest that the ELISPOT assay for IFN-γ is not a powerful tool to distinguish latent from active TB.

Although the pathology of tuberculosis has been accurately described for a long time, one of the problems is the difficulty in obtaining appropriate human lung tissue samples during a study (29). Furthermore, caseating granulomas are considered the characteristic lesions of all tuberculosis and the basis for "human-like" diseased animal models (30,31). One of the key advantages of the macaque model for *M.tb* research is that the entire spectrum of granulomatous lesions observed in human TB disease is presented (26). Following initial deposition of *M.tb* in the right lung lobe, early-stage macrophages and other immune cell infiltrates of lung tissue became organized as primary granulomas. At a later stage, the initiation of adaptive immunity led to the formation of different types of granulomas: solid, necrotic, and caseous granulomas,

which represented the dynamic interactions between *M.tb* and host defense (32). The pathological findings of TB disease in the macaque model were similar to those for humans, including pulmonary granulomas with or without calcification, caseation, cavitation, and infection of draining tracheobronchial lymph nodes (11,33,34). Our data demonstrated that *M.tb*-infected cynomolgus monkeys of Chinese origin developed granulomas with some unique features similar to humans (35), including centralized necrosis, multi-nucleated giant cells (known as Langerhans's giant cells), and lymphocytic cuff (lymphocyte-rich regions).

Type II alveolar cells are cuboid epithelial cells and function in maintaining the epithelial homeostasis and integrity through proliferation (36,37). Additionally, type II cell hyperplasia represents an important feature in the resolution and repair phase following lung injury, including intrapulmonary bacterial-induced alveolar epithelial injury in mice (38). The currently available data on the role of type II alveolar cells in *M.tb* infection come either from mice or human type II alveolar cell line (A549 cells) (39-42). In this study, we originally report that reactive type II cell hyperplasia was observed in animal WAP02 with active TB, indicating that type II cells might be involved in a repair mechanism following *M.tb* infection-induced alveolar injury. Notably, type II cell hyperplasia was located on the margin of the granuloma area, and the underlying mechanisms remain elusive. Therefore, the cynomolgus macaques may provide an opportunity to understand the role of type II alveolar cells in tuberculosis.

Conclusions

In summary, the results of this study indicate that cynomolgus macaques of Chinese origin can be used as an appropriate model for primary disease and latent infection. Because of the genomic, physiological, and immunological similarities to humans, the Chinese cynomolgus macaque model may represent the complete spectrum of granulomatous lesions that occurs in human TB disease. Our results showed that a subset of monkeys infected with 25 or 500 CFU of *M.tb* Erdman strain had no clinical signs of TB but were positive in TST and IFN-γ ELISPOT. These monkeys closely resembled the latent tuberculosis infection (LTBI). Because latent tuberculosis is difficult to model in animals, further investigations on pathogenesis of cynomolgus with latent infection should improve and advance our knowledge on how to reduce the risk of progression from LTBI to active disease.

3620

Zhang et al. TB infection of Chinese-origin cynomolgus macaques

Acknowledgements

Footnote

Conflicts of Interest: The authors have no conflicts of interest to declare.

Ethical Statement: The study manipulations and protocols were approved by the Institutional Animal Care and Use Committee of Wuhan University School of Medicine (IRB number: A32012012).

References

1. World Health Organization. Global tuberculosis report 2016, Available online: http://www.who.int/tb/publications/global_report/en/

2. Sharpe SA, McShane H, Dennis MJ, et al. Establishment of an aerosol challenge model of tuberculosis in rhesus macaques and an evaluation of endpoints for vaccine testing. Clin Vaccine Immunol 2010;17:1170-82.

3. Langermans JA, Andersen P, van Soolingen D, et al. Divergent effect of bacillus Calmette-Guerin (BCG) vaccination on Mycobacterium tuberculosis infection in highly related macaque species: implications for primate models in tuberculosis vaccine research. Proc Natl Acad Sci U S A 2001;98:11497-502.

4. Shen Y, Shen L, Sehgal P, et al. Antiretroviral agents restore Mycobacterium-specific T-cell immune responses and facilitate controlling a fatal tuberculosis-like disease in Macaques coinfected with simian immunodeficiency virus and Mycobacterium bovis BCG. J Virol 2001;75:8690-6.

5. Young D. Animal models of tuberculosis. Eur J Immunol 2009;39:2011-4.

6. O'Neil RM, Ashack RJ, Goodman FR. A comparative study of the respiratory responses to bronchoactive agents in rhesus and cynomolgus monkeys. J Pharmacol Methods 1981;5:267-73.

7. Carlsson HE, Schapiro SJ, Farah I, et al. Use of primates in research: A global overview. Am J Primatol 2004;63:225-37.

8. Scanga CA, Flynn JL. Modeling Tuberculosis in Nonhuman Primates. Cold Spring Harb Perspect Med 2014;4:a018564.

9. McMurray DN, Collins FM, Dannenberg AM Jr, et al. Pathogenesis of experimental tuberculosis in animal models. Curr Top Microbiol Immunol 1996;215:157-79.

10. Kaushal D, Mehra S, Didier PJ, et al. The non-human primate model of tuberculosis. J Med Primatol 2012;41:191-201.

11. Capuano SV 3rd, Croix DA, Pawar S, et al. Experimental Mycobacterium tuberculosis infection of cynomolgus macaques closely resembles the various manifestations of human M. tuberculosis infection. Infect Immun 2003;71:5831-44.

12. Walsh GP, Tan EV, dela Cruz EC, et al. The Philippine cynomolgus monkey (Macaca fasicularis) provides a new nonhuman primate model of tuberculosis that resembles human disease. Nat Med 1996;2:430-6.

13. Lin PL, Pawar S, Myers A, et al. Early events in Mycobacterium tuberculosis infection in cynomolgus macaques. Infect Immun 2006;74:3790-803.

14. Langermans JA, Doherty TM, Vervenne RA, et al. Protection of macaques against Mycobacterium tuberculosis infection by a subunit vaccine based on a fusion protein of antigen 85B and ESAT-6. Vaccine 2005;23:2740-50.

15. Green AM, Mattila JT, Bigbee CL, et al. CD4(+) regulatory T cells in a cynomolgus macaque model of Mycobacterium tuberculosis infection. J Infect Dis 2010;202:533-41.

16. Gormus BJ, Blanchard JL, Alvarez XH, et al. Evidence for a rhesus monkey model of asymptomatic tuberculosis. J Med Primatol 2004;33:134-45.

17. Zhang J, Xian Q, Guo M, et al. Mycobacterium tuberculosis Erdman infection of rhesus macaques of Chinese origin. Tuberculosis (Edinb) 2014;94:634-43.

18. Sharpe SA, Eschelbach E, Basaraba RJ, et al. Determination of lesion volume by MRI and stereology in a macaque model of tuberculosis. Tuberculosis (Edinb) 2009;89:405-16.

19. Krebs KC, Jin Z, Rudersdorf R, et al. Unusually high frequency MHC class I alleles in Mauritian origin cynomolgus macaques. J Immunol 2005;175:5230-9.

20. Zhang J, Ye YQ, Wang Y, et al. M. tuberculosis H37Rv Infection of Chinese Rhesus Macaques. J Neuroimmune Pharmacol 2011;6:362-70.

21. Guo M, Xian QY, Rao Y, et al. SIV Infection Facilitates Mycobacterium tuberculosis Infection of Rhesus Macaques. Front Microbiol 2017;7:2174.

22. Marsollier L, Andre JPS, Frigui W, et al. Early trafficking events of Mycobacterium ulcerans within Naucoris cimicoides. Cell Microbiol 2007;9:347-55.

23. Lin PL, Flynn JL, Tubearculosis research using Nonhuman primates, In: Abee CR, Mansfield K, Tardif S, et al., editors. Nonhuman Primates in Biomedical Research. London (United Kingdom): Academic Press, 2012:173-96.

24. Chen CY, Yao S, Huang D, et al. Phosphoantigen/IL2 Expansion and Differentiation of V gamma 2V delta 2 T Cells Increase Resistance to Tuberculosis in Nonhuman Primates. PLoS Pathog 2013;9:e1003501.

25. Barry CE III, Boshoff HI, Dartois V, et al. The spectrum of latent tuberculosis: rethinking the biology and intervention strategies. Nat Rev Microbiol 2009;7:845-55.

26. Lin PL, Rodgers M, Smith L, et al. Quantitative comparison of active and latent tuberculosis in the cynomolgus macaque model. Infect Immun 2009;77:4631-42.

27. Vincenti D, Carrara S, De Mori P, et al. Identification of early secretory antigen target-6 epitopes for the immunodiagnosis of active tuberculosis. Mol Med 2003;9:105-11.

28. Andrade Júnior DR, Santos SA, Andrade DR. Measurement of peripheral blood mononuclear cells producing IFN-gamma in patients with tuberculosis. Braz J Infect Dis 2008;12:123-7.

29. Hunter RL. Pathology of post primary tuberculosis of the lung: An illustrated critical review. Tuberculosis 2011;91:497-509.

30. North RJ, Jung YJ. Immunity to tuberculosis. Annu Rev Immunol 2004;22:599-623.

31. Russell DG, Barry CE, Flynn JL. Tuberculosis: What We Don't Know Can, and Does, Hurt Us. Science 2010;328:852-6.

32. Ehlers S, Schaible UE. The granuloma in tuberculosis: dynamics of a host-pathogen collusion. Front Immunol 2013;3:411.

33. Flynn JL, Capuano SV, Croix D, et al. Non-human primates: a model for tuberculosis research. Tuberculosis (Edinb) 2003;83:116-8.

34. Via LE, Lin PL, Ray SM, et al. Tuberculous granulomas are hypoxic in guinea pigs, rabbits, and nonhuman primates. Infect Immun 2008;76:2333-40.

35. Shaler CR, Horvath CN, Jeyanathan M, et al. Within the Enemy's Camp: contribution of the granuloma to the dissemination, persistence and transmission of Mycobacterium tuberculosis. Front Immunol. 2013 Feb 14;4:30.

36. Leslie KO. Lungs. In: Mills SE. ed. Histology for Pathologist. Philadelphia: Lippincott Williams & Wilkins Press, 2012:505-23.

37. Liu YR. Type II Cells as Progenitors in Alveolar Repair. In: Firth A, Yuan JX. Lung stem cells in the epithelium and vasculature. Springer, 2015:13-33.

38. Liu Y, Sadikot RT, Adami GR, et al. FoxM1 mediates the progenitor function of type II epithelial cells in repairing alveolar injury induced by Pseudomonas aeruginosa. J Exp Med 2011;208:1473-84.

39. Danelishvili L, McGarvey J, Li YJ, et al. Mycobacterium tuberculosis infection causes different levels of apoptosis and necrosis in human macrophages and alveolar epithelial cells. Cell Microbiol 2003;5:649-60.

40. Tomioka H. Type II pneumocytes in the evaluation of drug antimycobacterial activity. Expert Opin Pharmacother 2003;4:127-39.

41. Debbabi H, Ghosh S, Kamath AB, et al. Primary type II alveolar epithelial cells present microbial antigens to antigen-specific CD4+ T cells. Am J Physiol Lung Cell Mol Physiol 2005;289:L274-9.

42. Adlakha N, Vir P, Verma I. Effect of mycobacterial secretory proteins on the cellular integrity and cytokine profile of type II alveolar epithelial cells. Lung India 2012;29:313-8.